Journal of Theoretical and Computational Chemistry
© World Scientific Publishing Company

Effect of Molecular Solvents of Varying Polarity on the Self-Assembly of 1-n-Dodecyl-3-methylimidazolium Octylsulfate Ionic Liquid

Utkarsh Kapoor*
School of Chemical Engineering, Oklahoma State University,
Stillwater, OK 74078, USA
utkarsh.kapoor@okstate.edu

Jindal K. Shah†
School of Chemical Engineering, Oklahoma State University,
Stillwater, OK 74078, USA
jindal.shah@okstate.edu

Received Day Month Year
Revised Day Month Year
Accepted Day Month Year

Large scale molecular dynamics simulations consisting of more than 88,000-106,000 atoms are conducted to assess the effect of polar, nonpolar, and amphiphilic molecular solvents on the nanoscale structuring of the ionic liquid 1-n-dodecyl-3-methylimidazolium [C_{12}mim] octylsulfate [C_8SO_4] ionic liquid. Water, n-octane, and 1-octanol are employed as examples of polar, nonpolar, and amphiphilic molecules, respectively. The results indicate each of these molecular solvents modify the nanosegregation behavior of ionic liquids in a unique way. Water induces a high order of structuring of the ionic liquid as indicated by extremely high nematic order parameter for the system. In addition, the morphology of the neat ionic liquid is transformed from layer-like to that of a bilayer-like in which the polar and nonpoar domains alternate. The presence of water also causes the stretching of the nonpolar domain increasing its size. At the concentration examined in this work, n-octane is found to be only partially miscible with the ionic liquid. The polar network is maintained; however, the continous cationic nonpolar domain is split into multiple domains. n-Octane is accommodated in the ionic liquid nonpolar domain. Similarly, the amphilicity of 1-octanol leads to an increases in the number of cationic as well as anionic domains. The overall nonpolar domain length, however, remains nearly identical to that found for the pure ionic liquid. Additional characterization of structural features of the three systems is discussed in terms of 1-dimensional number densities, nematic order parameters for the overall systems and its components, and structure factors.

Keywords: Ionic liquids, Nanosegregation, Water, Structure Factor

---

[*] present
[†] Permanent address, Corresponding author

1. Introduction

Ionic liquids can be considered as non-aqeuous, highly concentrated electrolytes that are composed entirely of ions. Many ionic liquids are derived from an organic cation and organic/inorganic anion both of which agenerally possess low charge density rendering them liquids at room temperature. Essentially non-volatile in nature and the possibility to tune various thermophysical, chemical, and biological properties through an appropriate combination of cations and anions have led to tremendous research activities concerning ionic liquid over the last two decades. Researchers have demonstrated that ionic liquids are suitable for a large number of applications that range from gas absorption, reaction media, dissolution of cellulose for bioethanol production, electrolytes in dye-sensitized solar cells and Li-ion batteries, lubrication, and structure-directing agents for synthesis of ordered nanostructures such as zeolites.

It has been now established that many ionic liquids possess highly articulated nanophase segregated structures comprising of at least two domains: polar and non-polar. [1,2,3,4,5,6,7,8,9,10,11,12,6] Due to the presence of these domains in a single liquid, ionic liquids are sometimes referred to as "two-in-one" solvents [13] that are capable of dissolving polar, nonpolar and amphiphilic molecular solvents through their association with ionic liquid domains of matching polariy. In this context, ionic liquid and water mixtures have been investigated both experimentally[14,15,16,17,18,19] and using molecular simulation techniques.[20,21,22,23,24]. A comprehensive review of computational work dealing with ionic liquid-water mixtures is provided by Klein and co-workers. [25] These studies have demonstrated the mesocopic structure inherent to ionic liquids is preserved at low concentrations of water, and water preferentially interacts with the anion [26,27,28] and sometimes with the cation. [29] At intermediate concentrations, the continuous polar network of ionic liquid begins to collapse with the appearance of isolated clusters of ionic liquids. [30] At very high concentrations of water, formation of micelles,[31] isolated and dissociated ions pairs may be observed. [32] Recently, it was demonstrated that the temperature can disrupt the ionic liquid-water interactions to a greater extent than the water-water interactions in ionic liquid mixtures containing low and high water concentrations, respectively. [33] Water-induced structural transitions can have profound impact on the transport properties such as viscosity and ionic conductivity of the ionic liquid-water mixtures providing another avenue for tailoring the properties of ionic liquids.[34,35,36,37]

Alcohols are another class of molecular solvents that are capable of modifying ionic liquid properties. Owing to their amphiphilic nature and ability to act as both hydrogen-bond donor and acceptor, alcohols are expected to modify the molecular behavior in ionic liquids that is different from that of water. For example, increase in the alkyl chain on imidazolium-based ionic liquids leads to lowering of the upper critical solution temperature (UCST) for a given alcohol [38,39], while the solubility trend for water is exactly opposite. [40,41] As with water, the topic dealing with the effect of alcohols on the nanostructure of the ionic liquids has been pursued by many researchers, albeit to a lesser extent. Results from molecular simulations have suggested accumulation of -OH group of alcohols in the polar region of 1-n-alkyl-3-methylimidazolium [$C_n$mim] chloride Cl (n = 2, 4, and 6), while the alkyl chain is incorporated in the nonpolar domain. [42,43] In a concentration-dependent molecular dynamics study involving [C_4mim] tetrafluoroborate [BF_4] and its mixtures with water, methanol, and ethanol, the authors observed that the structural transitions were qualitatively similar. However, clusters of water molecules formed at low water concentrations while alcohol molecules were homogeneously distributed. [44] A number of experimental studies have been undertaken to elucidate structural modification (or lack thereof) when alchohols are dissolved in protic ionic liquids. [45,46]

The aforementioned studies focused exclusively on the influence of molecular solvents on ionic liquids for which the nonpolar content is present either on the cation or anion. Recently, we have demonstrated that the simultaneous presence of nonpolar moieties on both the ions ([$C_n$mim] octylsulfate [C_8SO_4]) can be leveraged as an effective strategy to transform nanostructure of ionic liquids from globular sponge-like for n= 2, 4, and 6 to layer-like for n = 8, and perforated layer-like for n = 10. Interestingly, when the cationic alkyl chain length is n-dodecyl, nanoscale structuring (polar-nonpolar-polar) is observed at multiple length scales. In this article, we examine the influence polar, nonpolar, and amphiphile molecules exert on the morphology of the [C_{12}mim][C_8SO_4] ionic liquid. We select water, 1-octanol, and n-octane as molecular solvents as examples of polar, amphiphilic, and nonpolar species. The choice of 1-octanol and n-octane is driven by the fact that the nonpolar domain is identical with that in the anion. In addition to probing the effect of a nonpolar molecular solvent such as 1-octane on the structural evolution in the ionic liquid, it should be emphasized that ionic liquids have been suggested as extracting agents for aromatics from alkanes. [47,48,49] Further, a recent investigation on liquid-liquid equilibria measurements of alkanes such as n-hexane, n-octane, and n-decane in an ionic liquid containing lipid-like appendage has shown, interestingly, a nearly temperature-independent solubility of these solvents in ionic liquid. The authors speculated that this behavior could arise from the dissolution of the nonpolar solutes entirely in the nonpolar domain of the ionic liquid.[50]

The next section of the article provides details on the force field employed for the ionic liquid as well as the solvents investigated in this study. Simulation protocols to generate well-equilibrated structures of the ionic liquid-solvent system are described in the Simulation Details section. As the focus of the present article is on the morphological evolution of ionic liquids in response to the solvents with which it is mixed, the Results and Discussions section is concentrated on the elucidation of the structures in terms of 1-dimension number densities, order parameter, and structure factors. The article ends with a summary of conclusions derived from this work.

2. Force Field

An all-atom force field developed by Canongia Lopes-Pádua [51,52] (CL&P FF) having the following functional form for computing intramolecular and intermolecular interactions:

$$\begin{aligned}E_{tot} = &\sum_{ij}^{\text{bonds}} \frac{k_{r,ij}}{2}(r_{ij} - r_{0,ij})^2 + \sum_{ijk}^{\text{angles}} \frac{k_{\theta,ijk}}{2}(\theta_{ijk} - \theta_{0,ijk})^2 \\ &+ \sum_{ijkl}^{\text{torsions}} \sum_{m=1}^{4} \frac{k_{m,ijkl}}{2}[1 + (-1)^{m+1}\cos(m\phi_{ijkl})] + \\ &+ \sum_{ij}^{\text{nonbonded}} \left\{ 4\epsilon_{ij} \left[\left(\frac{\sigma_{ij}}{r_{ij}}\right)^{12} - \left(\frac{\sigma_{ij}}{r_{ij}}\right)^{6} \right] + \left(\frac{q_i q_j}{r_{ij}}\right) \right\} \qquad (1)\end{aligned}$$

where $k_{r,ij}$, $k_{\theta,ijk}$, $k_{m,ijkl}$ represent the force constants for bond stretching, angle bending, torsion (both proper and improper), respectively, ϵ and σ indicate the Lennard-Jones 12-6 energy and size parameters, and q denotes partial charges; is a well parameterized and transferable force field that encompasses alcohols, alkanes, and imidazolium-based cations and sulfate-based anions with arbitrary chain lengths. Thus, 1-n-dodecyl-3-methylimidazolium $[C_{12}mim]^+$ cation and 1-n-octylsulfate $[C_8SO_4]^-$ anion, 1-octanol $[C_8H_{17}OH]$, and n-octane $[C_8H_{18}]$ were modeled using CL&P FF. Additionally, SPC/E model [53,54,55] was used for water $[H_2O]$ molecules. Geometric-mean combining rule was used to calculate unlike Lennard-Jones interactions. The intramolecular 1–4 nonbonded interactions were scaled by a factor of 0.5, however, such interactions were excluded for the atoms connected by bonds and angles. The total charge on the cation and anion is ± 1. The use of the CL&P FF in the current work would allow us to compare the results from the present work to those obtained in our previous work [56] for pure $[C_{12}mim][C_8SO_4]$ ionic liquid which was carried out with the same force field.

3. Simulation Details

Molecular dynamics (MD) simulations using GROMACS 4.5.5 package [57,58] were carried out at a temperature of 400 K and pressure of 1 bar. Three different mixture systems namely 1-n-dodecyl-3-methylimidazolium [C_{12}mim] 1-n-octylsulfate [C_8SO_4] ionic liquid (IL) – water [H_2O], [C_{12}mim][C_8SO_4] – n-octane [C_8H_{18}] and [C_{12}mim][C_8SO_4] – 1-octanol [$C_8H_{17}OH$] are presented in this work. Henceforth, the mixtures of [C_{12}mim][C_8SO_4] ionic liquid with [H_2O], [C_8H_{18}] and [$C_8H_{17}OH$] will be designated as IL:Water, IL:Octane and IL:Octanol, respectively.

It should be noted that the choice of 400 K temperature ensures liquid phase for n-octane and 1-octanol. Furthermore, the SPC/E water model [53,54,55] is known to predict liquid state for up to 400 K. All the simulated were conducted in a tetragonal simulation box with identical lengths in the x and y directions. Periodic boundary conditions were enforced in all the three dimensions. The initial configurations were prepared from a well-equilibrated cubic simulation box of the [C_{12}mim][C_8SO_4] ionic liquid containing 1000 ion pairs obtained from our previous work [56]. The configuration was placed at the base of the tetragonal supercell of xy-dimensions 93.5 Å × 93.5 Å. PACKMOL [59] was used to generate low density initial configurations for water, n-octane and 1-octanol using 3000, 1000 and 1000 molecules in the presence of ionic liquid molecules. Each of these configurations were placed in the empty space of the simulation box in the z-direction with identical xy-dimensions, which resulted in the z-dimension extending to 120 Å, 137 Å and 144 Å for IL:Water, IL:Octanol, and IL:Octane systems, respectively. As an example, the initial configuration setup for the IL:Water system is shown in Fig. 1. The number of solvent molecules were chosen such that ionic liquid and solvent molecules do not interact with their replicas along the z-direction.

The initial configurations were equilibrated in their respective phases by applying positional constraints and subjecting each of the two phases to steepest descent minimization to remove high energy contacts followed by a 2 ns annealing scheme, where the temperature of the system was iteratively raised from 400 K to 600 K linearly in 200 ps followed by canonical (NVT) ensemble equilibration at 600 K for 100 ps and then brought down linearly to the desired temperature of 400 K in the next 200 ps. Additional relaxation of the system was achieved by simulating the systems in the NVT ensemble for 40 ns after which the constraints were removed and mixing of the two phases was allowed to occur. To ensure that the reported quantities were obtained for well-equilibrated structures, an extensive equilibration protocol was adopted. The equilibration was done in four stages; a cycle comprising of an annealing scheme for a duration of 2 ns, using the same protocol as above, and NVT and isothermal-isobaric (NPT) ensemble equilibration runs of 10 ns and 20 ns respectively was repeated three times. In the final cycle, the system was subjected to a 10 ns annealing scheme followed by NVT and NPT ensemble equilibration runs of 20 ns and 40 ns, respectively. After this, 40 ns of NPT ensemble production run was conducted. The convergence was validated based on density and total energy equilibration. The trajectories obtained from the final 10 ns were used for the structural analysis presented below.

All the simulations were performed with a time step of 0.002 ps, and the coordinates were saved every 50 ps. Appropriate tail corrections were applied for non-bonded LJ interactions while electrostatic interactions were handled using PME method, each with a potential cutoff of 16 Å. Nosé-Hoover thermostat was used to control the temperature with a coupling constants of 0.4 ps. Semi-isotropic pressure coupling with a coupling constant of 2.0 ps was used for the xy- and z-dimension separately using Parrinello-Rahman barostat. The choice of semi-isotropic pressure coupling over isotropic coupling was influenced by the fact that pure $[C_{12}mim][C_8SO_4]$ ionic liquid exhibits a layer-like structural morphology as shown in our previous study. [56]

4. Results and Discussion

The results below are provided in terms of the polar and nonpolar groups present in the [C_{12}mim][C_8SO_4] ionic liquid, [H_2O] water, [C_8H_{18}] n-octane, and [$C_8H_{17}OH$] octanol. We will use cation-polar to refer to the polar group containing the imidazolium ring as well as the methyl and methylene groups directly bonded to the ring. Similarly, anion-polar represents sulfur and oxygen atoms, and the methylene group attached to oxygen in octylsulfate. The octanol-polar group contains the hydroxyl and the methylene group attached to the oxygen in 1-octanol while water is completely polar. The nonpolar regions in the cation, anion, 1-octanol and n-octane are indicated by the uncharged carbon groups while the terms cation-tail, anion-tail, octanol-tail and octane-tail denote the terminal carbon atom of the alkyl chains, respectively. A schematic is provided in Fig. 2.

Structural properties of the ionic liquid systems are described in terms of structure factors, number density, radial distribution functions, and orientational order parameter. The structure factors were calculated using STRFACT [60]; number density was computed using density profile tool for VMD [61]. The radial distribution functions and domain analysis included in the supporting information[§] were analyzed using the tools implemented in TRAVIS. [62,63] while the configuration snapshot visualization was rendered using VMD [64]. The orientational order parameter was obtained using MDTraj. [65] The aggregate size distributions were analyzed using AGGREGATES. [66]

4.1. *Simulation Snapshots*

Imidazolium-based ionic liquids with long chain substituents possess segregated polar and nonpolar domains independent of the anion identity. [67,2,68,69,70,4,71,72] Our previous study has shown that [C_{12}mim][C_8SO_4] ionic liquid system exhibits a layer-like structure that is characterized by the presence of biphasic regime (polar and nonpolar domains) with different types of ionic sublayers. [56] In an effort to visualize and understand the influence of polar and nonpolar solvents such as water, n-octane and 1-octanol on the morphology of [C_{12}mim][C_8SO_4] ionic liquid system, we present in, Fig. 3, a static snapshot of the configurations obtained at the end of the equilibration. The rendering scheme employed for the ionic liquid is consistent with our previous study [56]: cation-polar in red, anion-polar in yellow, cation-nonpolar in green and anion-nonpolar in blue while water and n-octane are depicted in purple and orange, respectively. Furthermore, the polar and nonpolar groups for 1-octanol are represented in silver and pink, respectively. The coloring scheme is also shown in the chemical structure schematic (Fig. 2).

Fig. 3(a) shows that the presence of water dramatically alters the morphology of the pure ionic liquid system such that there is nearly a complete segregation of polar and nonpolar domains, which resembles that of an alternating lipid bilayer-like structure. The observed changes, upon dilution with water, is different from the transformation of a $[C_{10}mim]Br$–water mixture from lamellar phase to a hexagonal columnar phase as the water mole fraction is increased from 11-16 % to more than 40 %. [73,74] Such a difference can be attributed to the presence of longer alkyl chain length in the cation and octyl moiety in the anion. Additionally, water is almost exclusively located in the polar region, which is consistent with a number of previously available reports. [75,76,77,78] A few water molecules are found to penetrate into the nonpolar region, probably due to thermal fluctuations. Although the formation of a number of water clusters is visible in the snapshot, instances of isolated water molecules do exist as evidenced in Fig. S3(a) of the supporting information[§]. Fig. 3(b) indicates that the continuity of the polar domain present in the neat ionic liquid is nearly destroyed. However, the domain count and aggregate analysis included in Figs. S2 and Fig. S3 (a) of the supporting information[§] suggest the preservation of the continuous polar network constituted by the cation-polar and anion-polar groups.

Fig. 3(c) shows the structural morphology of the IL:Octane system. In agreement with other studies, [79,1] it is observed that n-octane interacts preferentially with the nonpolar domain of the ionic liquid. The simulation snapshot also reveals that not all the molecules of n-octane are interspersed in the ionic liquid, indicating only partial immiscibility of the ionic liquid-n-octane system at the concentration examined in this study. Though not immediately evident from the two-dimensional representation in Fig. 3(e), the network developed between the chains of n-octane is not continuous based on the number of domains obtained for the solvent (Figs. S2 and S4 of the Supporting Information.[§]). The polar network of the ionic liquid is maintained along with its morphology of the neat ionic liquid system, [56] which is provided in Fig. 3(d). Thus, the layer-like morphology of ionic liquid is mostly retained. On the other hand, due to the swelling of nonpolar domains of the ionic liquid, polar network is stretched making the polar strands appear thinner as compared to the pure ionic liquid or IL:Water system. The dissolution of n-octane also leads to the loss in the connectivity of the cationic nonpolar domain of the ionic liquid. Further, the number of nonpolar domains contributed by the anion also increases (Fig. S2) providing additional evidence that n-octane localizes in the nonpolar domain of the ionic liquid. Increase in the number of nonpolar domains can also be taken to indicate that the solubilization of n-octane is entropically driven as suggested by Greaves and Drummond based on the increase in the solubility of ethane and butane with increase in the alkyl chain length of $[C_n mim][NTf_2]$ ionic liquid. [80]

Fig. 3(f) and (g) illustrate the morphology of the IL:Octanol system, and its continuous polar domain (Figs. S2 and S5 of the supporting information[§]) respectively. It is evident that the amphiphilic nature of 1-octanol changes the morphology of both polar and nonpolar domain with enhanced structuring and layer-like connectivity. The polar domain appears denser than what is observed for the pure ionic liquid system suggesting that more cation- and anion-heads are involved to maintain continuity of the polar domain. It may be inferred that 1-octanol is more soluble than n-octane as there is no evidence of a separate 1-octanol bulk-like phase in the system. Fig. S2 of the Supporting Information provides additional insight into the morphological changes occurring in the ionic liquid system. The single cationic non-polar domain in the neat ionic liquid is now split into multiple domains. The increase in the number of anion-polar domains is even more dramatic. The two observations point to significant perturbations in the nonpolar domain of the ionic liquid induced when 1-octanol is dissolved in the ionic liquid. Multiple domains for 1-octanol polar and nonpolar groups are evidence that 1-octanol is distributed throughout the system.

It is worth mentioning that the visual comparison of Fig. 3(a) and (f) also suggests that the morphological model observed can be compared with the structural model proposed by Cruz et al. [81] for n-alkylpyridinium n-alkylsulfate in which the authors suggested a presence of double ionic layer with no interdigitation vs. single ionic sublayer with partial interdigitation of nonpolar chains or its combination. Thus, IL:Water system seems to possess double ionic layer polar domain with no interdigitation of terminal carbon of the alkyl chains while IL:Octanol system has partial interdigitation of nonpolar chains with less intermeshed polar domain.

4.2. *Orientational Order Parameter*

The degree of orientational order can be characterized using nematic order parameter, which can be computed through traceless and symmetric Maier-Suape [82,83] second rank ordering tensor (eq. 2)

$$Q_{\alpha\beta} = \frac{1}{N_m} \sum_{i=1}^{N_m} \left(\frac{3}{2} \hat{u}_{i\alpha} \hat{u}_{i\beta} - \frac{1}{2} \delta_{\alpha\beta} \right) \tag{2}$$

where α and β are the Cartesian indices, $\hat{u}$ is the unit vector associated with each molecule along its molecular axis, N_m is the number of molecules, δ is the Kronecker delta function. The nematic director (preferred orientation direction) and the order parameter are associated with the eigenvectors of the diagonalized $Q_{\alpha\beta}$. The order-parameter takes values between 0 for randomly oriented to 1 for perfectly aligned molecules. The significance of such orientational correlations have also been observed for the broad class of liquid crystals where the usual order-parameter range is 0.3–0.8. [84,82]. It is also interesting to note that the nematic order-parameter can be measured using X-ray or neutron scattering techniques by coupling the orientational and positional orders of the scattering moieties. [85] Furthermore, this approach can be considered as an alternate to the director obtained using second Legendre polynomial definition along a particular direction which has proved useful for analyzing self-assembly of ionic liquids in the past studies. [?,86,87,88]

In this work, the order parameter has been analyzed considering each moiety, i.e., the ionic liquid cation and anion, solvents (water, octane, 1-octanol) separately along with the overall order parameter for the ionic liquid:solvent system. Fig. 4 presents the calculated nematic order parameters for pure ionic liquid, IL:Water, IL:Octane, and IL:Octanol systems. Considering the pure ionic liquid, the order parameters for both the cation and anion and the overall system are similar with values $\sim$0.25, which is less than the value usually observed for liquid crystals. Rather low values for the nematic order parameter is indicative of the fact that there exists no preferred alignment direction for the cations and anions as can also be observed in the simulation snapshot. Nonetheless, nearly identical values for the cation and anion nematic order parameter suggest high ordering among the cationic and anionic nonpolar chains due to the alternating placement of cations and anions as advocated by the RDFs (supporting information) and structure factor analysis (see below). This is also the primary reason that the order parameters for the cation and anion are almost identical for all the systems studied in this work.

In comparison to pure ionic liquid system, the presence of nonpolar solute such as n-octane does not alter the extent of ordering in the cation and anion significantly. Moreover, there is no preferential ordering among octane molecules as indicated by a low order parameter ($\sim$ 0.2). This behavior is expected as the ionic liquid and n-octane are only partially miscible at the molar ratio considered in this work, which leads to octane occupying and only the nonpolar region of the ionic liquid and swelling the region. However, the overall polar domain remains nearly unaltered. The result is further confirmed by the simulation snapshot and the number density profiles, *vide infra*.

The presence of amphiphilic alcohol such as 1-octanol, on the other hand, significantly influences the alignment of ionic moieties as reflected in the order parameter changing from 0.25 to 0.55 indicative of highly ordered crystalline behavior. It is also noteworthy that the orientational order for 1-octanol itself is very low, which signifies that the presence of 1-octanol serves to modify the morphology of the ionic liquid. Addition of a polar species such as water leads to a high degree of ordering of the ionic liquid ions, as compared to the nonpolar octane or the amphiphilic 1-octanol. The order parameter for the ion moieties is as high as 0.78 suggesting that order is at the limit of liquid crystalline behavior range. The alignment is clearly visible in the simulation snapshot, Fig. 3 (a), which shows that the liquid crystalline behavior arises due to the orientation of nonpolar chains of the ionic species along a common director. On the contrary, the nematic order parameter for water is much lower. In fact, it is the least among the three solvents investigated here, which is due to the fact that, being a small molecule, the orientation of the longest molecular axis of water is randomly distributed lowering the overall nematic order parameter when water is included in the analysis.

Our analysis demonstrates that, for ionic liquids,such as [C_{12}mim][C_8SO_4] possessing high amphiphilic character and an inherent property to self-aggregate, the structural features can be dramatically altered by modulating the interactions in the ionic liquid polar domain.

4.3. *1-Dimensional Atomic Densities*

In order to provide additional insight into the arrangement of polar and nonpolar groups of the ionic liquid and solvent molecules, number density, along the longest axis - the z-coordinate, was computed using the density profile tool developed by Giorgino [61]. Figs. 6(a)-(d) represent these calculations for pure IL, IL:Water, IL:Octane and IL:Octanol systems, respectively. It should be noted that, due to layer-like morphology evolution in the IL:Water system, the system was aligned in such a way that the polar layer is perpendicular to the z-direction, as shown in Fig. 5. Previous studies [89,86,56] have employed similar analysis to deduce the formation of layer-like phases in spatially heterogeneous amphiphilic systems.

For the pure ionic liquid system (Fig. 6 (a)), the number densities for the polar groups of the both ions are periodic in nature with the same phase. Similar observations can be made for the number densities for the nonpolar groups of both the ions. However, the polar and nonpolar groups of a given ion exhibit densities that are out of phase further confirming the layer-like morphology that exists in the pure ionic liquid system. The non-zero number densities along the z-axis for all the groups indicate that although the polar and nonpolar groups alternate, they coexist in a given plane, which is also evident from the simulation snapshot. Additional structural characterization of pure IL system can be found in our previous study. [56]

The number density plots provided in Fig 6 (b) show that, similar to the pure ionic liquid system, the polar regions in the IL:Water systems are segregated by the nonpolar region. However, the peaks and valleys for the distributions of each of the moieties are remarkably well resolved as compared to those in Fig. 6 (a). Consistent with the morphology presented in Fig. 5, four polar domains can be clearly identified based on the number of maxima for the polar groups. Each of the polar domains is characterized by a single peak for water molecules and bimodal distributions for the cation-polar and anion-polar groups. The peak location for the water molecules coincides with the depression in the number densities for the cation- and anion-polar groups, indicating that water molecules are primarily at the center of the polar domain bridging the cation and anion interactions. Due to the polar nature of water, the maximum in the number density is achieved when the densities of the nonpolar groups are zero. Wider distributions of the anion-polar densities than those of the cation-polar suggests that the anions are positioned on the outer edge of the polar domain. Similarly, nonpolar regions of the cation and anion oscillate together. Each nonpolar domain contains a bimodal distribution for the anion-nonpolar densities, which arises from the octyl chains contributed by the anions from opposite faces of the adjoining polar domains. On the other hand, a unimodal distribution for the cation-nonpolar groups is obtained. In addition, the distance between the peaks of successive cation-nonpolar domains is ∼35 Å while the two peaks in the same bimodal distribution for anion-nonpolar groups are ∼15 Å apart. Also, the distance between both cation-nonpolar domains and respective polar domain peaks is ∼35 Å. This analysis provides an indication of the domain lengths observed the in IL:Water system. It is also worth mentioning that the absence of cation and anion-polar groups in the region over which the nonpolar domain peak is observed further confirms periodic alternation in the polar and nonpolar domains.

Fig. 6 (c) displays the number density distributions for various groups for the IL:Octane system. The general features of cation and anion polar and nonpolar components of ionic liquid are very similar to that observed in Fig. 6 (a) suggesting that the layer-like structure of the neat ionic liquid is more or less preserved. The only major difference in the nonpolar number densities is that associated with the region between 20 Å and 45 Å where the distribution is more isotropic due to the presence of octane in the vicinity suggesting the possibility for changes in the nonpolar domain. The density peak for n-octane at ∼ 110 Å with a distribution spanning over 60 Å (80-140 Å z-distance) arises due to partial miscibility of the ionic liquid and n-octane. Over this region, the probability of finding polar groups is negligible.

Similar to the systems mentioned above, the IL:Octanol system also depicts oscillatory behavior in the number densities for the polar and nonpolar groups. However, notable differences between the IL:Water and IL:Octanol systems can be observed in Fig. 6 (d). For example, the number densities for the cation-polar and anion-polar groups do not vanish at any point along the z-axis, which points to a continuity in the ionic liquid polar domain as with the pure ionic liquid system. Thus, at least on the simulation time scales sampled in this work, the addition of 1-octanol does not transform the morphology of the pure ionic liquid system to that resembling a truly layer-like morphology. Such a behavior is possibly due to the affinity of 1-octanol for the ionic liquid polar region to maximize interactions through -OH moiety and also the partitioning of the octyl chain in the nonpolar domain. The overall effect appears to be the accommodation of 1-octanol in the pure ionic liquid system. The presence of bimodal distributions in the number densities for the anion-nonpolar and 1-octanol can be taken as a signature of a length scale that is ∼15 Å. A longer length scale (∼32 Å) established from the separation of the successive cation-polar peaks is shorter than the one that is formed in the IL:Water system. Nonetheless, aggregation at multiple length scales is present in the IL:Octanol system.

The number density analysis clearly indicates that a greater degree of structuring of the ionic liquid can be induced in the presence of polar and amphiphilic solutes, providing an additional avenue to fine-tune the nanostructure of ionic liquids.

4.4. *Structure Factors*

The total structure factor, $S(q)$, was calculated from $S(q) = \sum\limits_i \sum\limits_j S_{ij}(q)$, where $\mathrm{S}_{ij}(q)$ is the partial structure factor obtained from the Fourier transform of the radial distribution function, $g_{ij}(r)$, between the atoms of type i and j. In particular, $S_{ij}(q)$ is given by:

$$S_{ij}(q) = \frac{\rho_o x_i x_j b_i(q) b_j(q) \int\limits_0^R 4\pi r^2 \left[g_{ij}(r) - 1\right] \frac{\sin\,(qr)}{qr} \left(\frac{\sin\,(\frac{\pi r}{R})}{\frac{\pi r}{R}}\right) dr}{\left[\sum\limits_i x_i b_i(q)\right]^2} \tag{3}$$

In eq. 3, q is the scattering vector, ρ_o is the average atomic number density, x_i is the atomic fraction of i, and and $b_i(q)$ is the coherent bound neutron scattering length of the atomtype i interpolated from the values in International Tables for Crystallography, Vol C. [90] R represents the cutoff distance defined for calculating $g_{ij}(\mathrm{r})$. A Lorch type window function, $\left(\frac{\sin(\frac{\pi r}{R})}{\frac{\pi r}{R}}\right)$ in eq. 3, is also used to attenuate the effect of using finite cutoff in $g_{ij}(\mathrm{r})$ calculations. [91] The total and partial structure factors were computed using STRFACT [60]. The cutoff distance, R, for these calculations was set equal to the half of the simulation box length in the x direction (due to the elongation of the box along the z-axis, the dimensions for the x and y axes are smaller than that for the z-axis). In order to avoid spurious effects, all the structure factors were truncated at the reciprocal q-value corresponding to the half of the box length in the x direction.

The structure factor obtained for all the systems studied in this work are included in Fig. 7. To enhance the visual clarity and precisely identify the peak locations, the structure factors for IL:Water, IL:Octane and IL:Octanol are offset along the y-axis. All the structure factors exhibit a well defined peak at q = 1.42 $\mathrm{\AA}^{-1}$ due to the juxtaposition of cations and anions, a shoulder around q = 1 $\mathrm{\AA}^{-1}$ signifying the charge alternation (cation-anion-cation and anion-cation-anion arrangement) within the polar network, and a pre-peak in the low-q region, q $\leq$ 0.2 $\mathrm{\AA}^{-1}$, representing a length scale associated with alternating polar and nonpolar domains. An extra peak at around q = 0.38 $\mathrm{\AA}^{-1}$ is seen to develop for the IL, IL:Water, and IL:Octanol, which is absent for the IL:Octane system. The first three peaks are general features for ionic liquids that form polar and nonpolar domains, which have been reported for a range of ionic liquids. [72,92,93,12,94,86,56]. It is worth mentioning that the appearance of a small shoulder at q = 1 $\mathrm{\AA}^{-1}$ is due to the cancellation of the same-type (cation-cation and anion-anion) and opposite-type (cation-anion) interactions and not because the charge alternation symmetry is absent. [56,87,12] The periodic nature of same-charge and opposite-charge species is also supported by RDFs included in the supporting information§. Further, the small peak, at around q = 0.38 Å^{-1}, between pre-peak and intermediate-q shoulder is representative of the ionic liquid nanostructure at multiple length scales, which was observed and reported by us for the pure ionic liquid recently. [56] A detailed explanation regarding the structure factor for [C_{12}mim][C_8SO_4] can be found in our previous study [56]. As already mentioned, for pure ionic liquid the peak attributed to adjacent organization of ionic moieties arises at q = 1.42 Å^{-1}. It is interesting to note that presence of solvent such as water, n-octane and octanol influences the organization of ions within the polar network. Such subtle rearrangement is suggested by shifting of the adjacency peak to q-values namely, 1.41 Å^{-1}, 1.41 Å^{-1} and 1.43 Å^{-1} for IL:Water, IL:Octane and IL:Octanol mixture systems, respectively. Thus, the presence of solutes (polar, nonpolar or amphiphilic) species leads to a subtle reorganization of ion moiety in the first solvation shell of the ionic liquid ions. This behavior is also corroborated by the RDFs presented in the supporting information§ (Figs. S6, S7 and S8 respectively). Similar displacements of the adjacency peak were observed in our previous study [56] due to an increase in the cationic alkyl chain length that modifies that aggregation behavior of the alkyl chains in the nonpolar domain and hence, the organization of the cation-anion polar groups.

The location of the pre-peak for IL:solvent mixture systems exhibit an interesting behavior. The pre-peak for the pure ionic liquid occurs at q = 0.19 Å^{-1} indicating a reciprocal space length of ∼ 33 Å. [56] For IL:Water mixture system, the nonpolar domain length across the layer-like polar domain is ∼ 37 Å corresponding to the pre-peak q value of 0.17 Å^{-1}. The elongation of the nonpolar domain can be explained on the basis of the observation that the partial interdigitation of the dodecyl chains emanating from the opposite faces of the adjoining domain vanishes, and the cationic nonpolar tails align end-to-end with high order increasing the nonpolar domain length. Further, the analysis of the distances between the various peaks in the number density plot (Fig. 6 (c)) reveals that the length scale associated with the pre-peak can be attributed to the cationic nonpolar-polar domain - cationic nonpolar domain arrangement and also the cationic nonpolar - polar - anionic nonpolar-anionic nonpolar domains. The polar-nonpolar-polar arrangement also gives rise to distances that are consistent with the pre-peak location. Similarly, for IL:Octane, the shifting of the pre-peak to lower-q values can be anticipated, as n-octane favorably resides in the nonpolar domain that causes the ionic liquid nonpolar domain to swell, thus increasing the distance between two polar strands. Therefore, q-value associated with pre-peak of IL:Octane is 0.13 Å^{-1}. However, this result should be interpreted with caution as complete mixing of n-octane and the ionic liquid did not occur over the course of the simulation. It is interesting to note that the addition of amphiphilic specie, such as 1-octanol, affects the nonpolar domain length only subtly (domain length ∼ 32 Å) and can be rationalized in terms of intermeshing of the cationic alkyl chains. Similar observation was reported by Drummond and co-workers in their study involving the nanostructure characterization of protic ionic liquids and their mixtures with n-alcohols. Based on the small and wide angle X-ray scattering data, the authors concluded that the nonpolar domain length was not affected when the alkyl chain of alcohol matched with that of protic ionic liquid, for example butanol and butylammonium nitrate. [45] Thus, increasing both polar and nonpolar content in the system do not necessarily increase the overall length of the nonpolar domain; however, structural ordering of the system can be greatly impacted as shown in Fig. 4.

A small peak between pre-peak and intermediate-q shoulder is clearly visible for all the systems studied in this work except for IL:Octane. As mentioned earlier, such peak signifies nanostructure over multiple length scales. For the pure ionic liquid system (also shown in our previous study [56]) such peak appears at q = 0.39 Å^{-1}. Addition of water to the ionic liquid not only increases the intensity of the peak but also shifts it to slightly lower q value of 0.38 Å^{-1}. In fact, another small shoulder arises at q = 0.54 Å^{-1} (real space length of 11.6 Å) which is absent in the case of pure ionic liquid. The origin of these peaks can be traced to the RDFs of the IL:Water system provided in the Supplementary Information (Fig. S6 (a) and (b)), especially that of cation polar-anion polar and those involving tail carbon atoms. The cation polar-anion polar RDF is marked by a second peak maximum at approximately 11.2 Å, thus it is likely that the ions in the second solvation shell contribute to the appearance of the shoulder at q = 0.54 Å^{-1}. Given that 11.2 Å is shorter than the separation between the two polar domains, the peak is related to the ions found in a given polar domain. Although the second solvation shell maximum in the cation-anion polar RDFs occurs at roughly the same distance for $[\text{C}_{12}\text{mim}][\text{C}_8\text{SO}_4]$, the absence of the shoulder at q = 0.54 Å^{-1} is probably related to low structuring in the system (nematic order parameter of 0.25 vs. 0.78 for the IL:Water system). For IL:Octane system, this secondary peak is not present. This behavior can be expected based on the analyses presented above, as n-octane resides in the nonpolar domain causing it to swell and not allowing the terminal carbon chains to interact effectively and rearrange heterogeneously, which eventually can lead to nanostructure over multiple length scales. However, for IL:Octanol system, such peak appears at q = 0.40 Å^{-1}. It is interesting to note that the ratio of pre-peak to this peak can be indexed to 1:2, which is consistent with the structural model suggested by Cruz et al. [81], thereby suggesting formation of different type of micro-domains that are continuous.

In order to further dissect and interpret the influence of various polar and nonpolar solvents on the morphology of ionic liquid, the partial structure factor for the ionic liquid was calculated, which was subsequently partitioned on the basis of polarity. The decomposition is shown in Fig. 8, where cation-head and anion-head are polar, and uncharged carbon chains on both cation and anion are nonpolar in nature. General features of the partial structure factors for the pure ionic liquid, IL:Water and IL:Octanol are that the pre-peak and the intermediate peak ($q \sim 0.38$ Å $^{-1}$) are a net result of two peaks and one antipeak at the respective reciprocal wave vectors. The in-phase peaks refer to the correlations due to the same polarity partitioning (polar-polar and nonpolar-nonpolar). On the other hand, the anti-peak is ascribed to the alternation in the polar and nonpolar domains. [86,95] In contrast to other systems, IL:Octane system shows a very complex behavior. Fig. 8(c) displays a peak for polar-polar interactions at same q value where pre-peak is visible for IL:Octane system (Fig. 7). However, the long range peak for nonpolar-nonpolar region is not present. We believe that this is due to n-octane occupying location in the nonpolar domain and forming nonpolar domain that is larger than the cutoff employed to calculate the structure factor. As a result of this truncation, both the nonpolar-nonpolar and polar-nonpolar cross interactions peaks are affected. The characteristics for the polarity partitioning for the structure factors for the IL:Solvent systems provided in the supplementary information (Fig. S1) are similar to those found for the ionic liquid.

5. Conclusion and Outlook

Molecular dynamics simulations containing 1-n-dodecyl-3-methylimidazolium [C_{12}mim] 1-n-octylsulfate [C_8SO_4] ionic liquid (IL) mixed with (i) water [H_2O], (ii) n-octane [C_8H_{18}], and (iii) 1-octanol [$C_8H_{17}OH$] were carried out at 400 K with the objective of determining the influence of polar, nonpolar and amphiphilic solute species on the nanostructural morphology of the ionic liquid. Large simulation boxes containing 1000 molecules for each species except water (3000 molecules) were used to probe the long length scale structures anticipated in these ionic liquids. The structural properties of the ionic liquid-solvent system were analyzed in terms of the structure factors, nematic orientational order parameter, and number densities along the longest axis.

Visualization of instantaneous simulation snapshots for these systems indicated different effects of the solvents on the underlying ionic liquid structure. IL:Water system shows a highly ordered double ionic layer-like morphology with the absence of nonpolar chains interdigitation, while IL:Octanol system represents similar layer-like morphology, albeit less ordered, with polar domain less intermeshed and partial interdigitation of alkyl chains, thus suggesting shorter layer spacing. On the other hand, octane does not influence the morphology of the ionic liquid to a greater extent due to its partial miscibility with the ionic liquid at the concentration probed in the study. Analysis of the number density distributions revealed that water and 1-octanol result into a sharper bimodal distribution for the anion nonpolar chain, which potentially leads to nanoscale segregation at multiple length scales. Interaction of the ionic liquid and solvents also produce a high degree of structuring, especially for the IL:Water and IL:Octanol systems. The total structure factors calculated for these systems share common features: pre–peak, intermediate–q shoulder and the adjacency peak, revealing microphase separation between the polar and nonpolar domains. Furthermore, existence of peaks between pre–peak and intermediate–q shoulder was also observed suggesting nanoscale heterogeneity over multiple lengths. However, it remains to be seen that if the peak persists when simulations with timescales much longer than probed in this work are carried out. Such a calculation is warranted to unequivocally eliminate the effect of the sluggishness of the system when CL&P force field is employed. Nonetheless, It was found that the peak becomes more evident with increase in the orientational order of the ionic moieties. In fact, multiple peaks between the pre–peak, intermediate–q shoulder are obtained for the IL:Water system.

In summary, the use of polar and amphiphilic species provides an additional approach to tailor ionic liquid morphologies. We are currently exploring this strategy to assess changes in the morphology for ionic liquid mixtures differing in amphiphilicity as a function of concentrations.

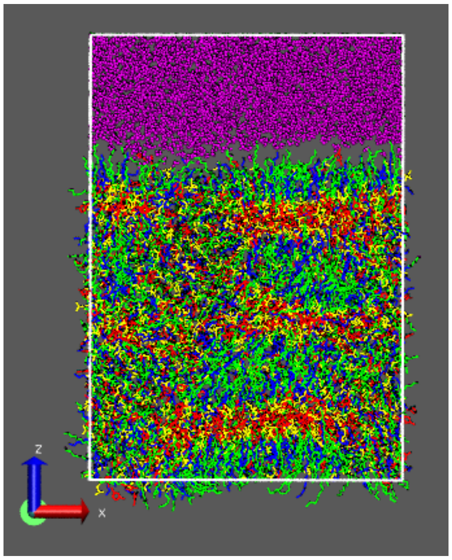

Fig. 1. Initial configuration setup for ionic liquid and water mixture systems. The snapshots is color-coded to reflect presence of polar and nonpolar components (Cation-polar: red, Anion-polar: yellow, Cation-nonpolar : green, Anion-nonpolar: blue, Water: purple). The tetragonal box dimensions are 93.5 Å × 93.5 Å × Å.

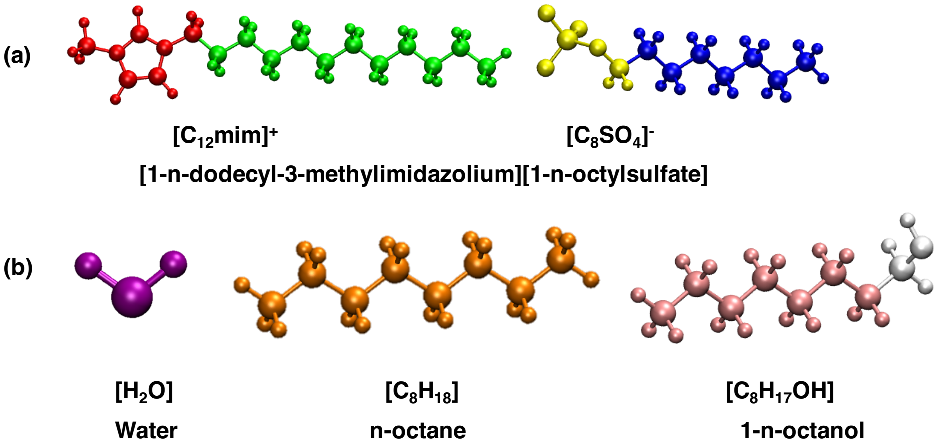

Fig. 2. Chemical structure of (a) 1-n-dodecyl-3-methylimidazolium $[C_{12}mim]^+$ and 1-n-octylsulfate $[C_8SO_4]^-$ ions comprising the ionic liquid, color coded to depict polar and nonpolar parts; (b) Solvents: water $[H_2O]$, n-octane $[C_8H_{18}]$, 1-octanol $[C_8H_{17}OH]$ color coding used to render the instantaneous simulation snapshots.

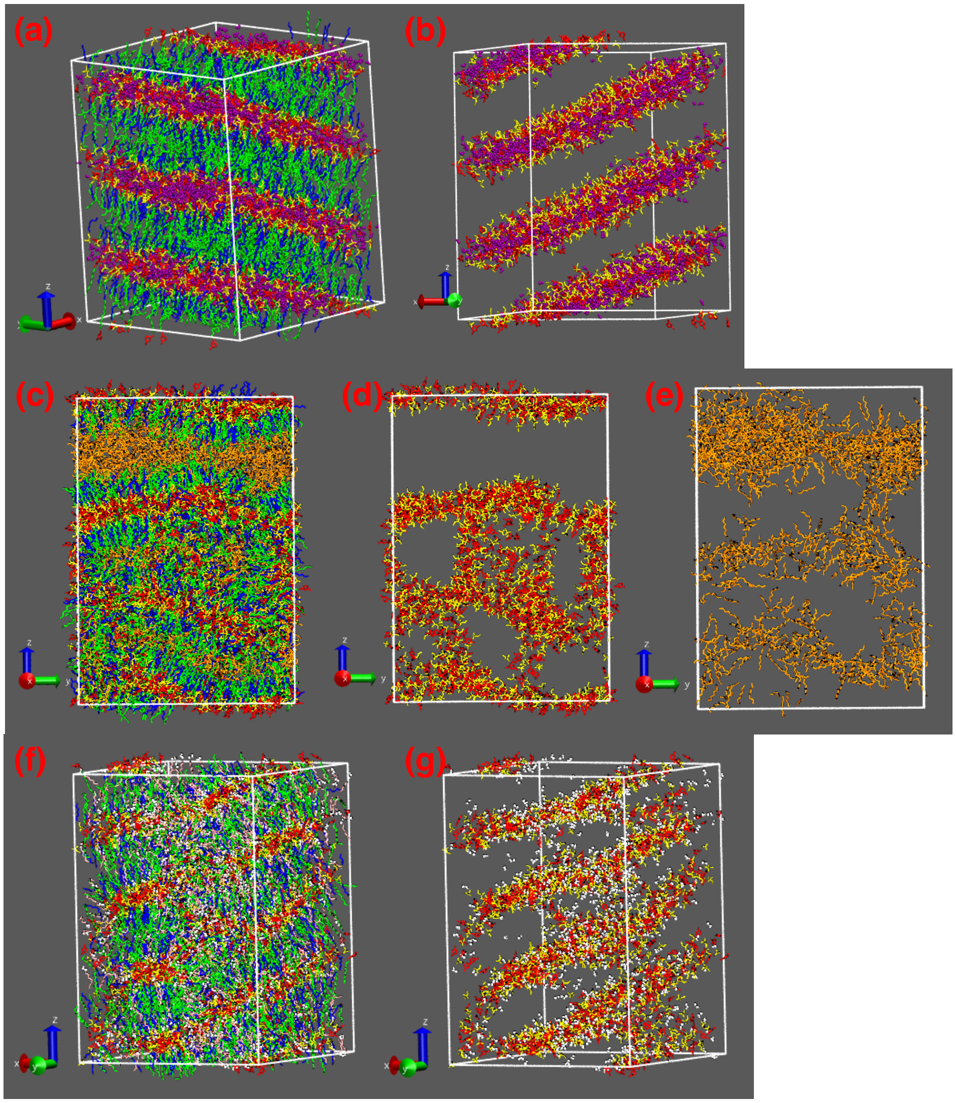

Fig. 3. Instantaneous snapshot of the equilibrated systems (a) IL:Water (b) IL:Water (only polar domain); (c) IL:Octane (d) IL:Octane (only polar domain) (e) IL:Octane (only octane); (f) IL:Octanol and (g) IL:Octanol (only polar domain). The snapshots are color-coded to reflect various polar and nonpolar components (Cation-polar: red, Anion-polar: yellow, Cation-nonpolar : green, Anion-nonpolar: blue, Water: purple, Octane:Orange, Octanol-polar: Silver and Octanol-nonpolar: Pink)

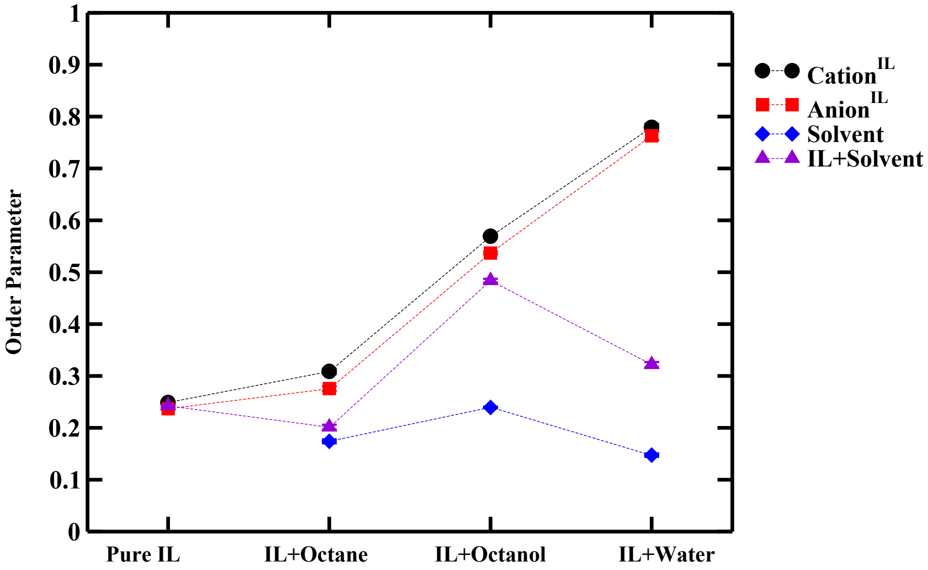

Fig. 4. Orientational order parameter for pure [C_{12}mim][C_8SO_4] IL, IL:Octane (c) IL:Octanol (d) IL:Water systems decomposed into cations and anions comprising the ionic liquid, solvent and IL + solvent (overall) mixture systems. Please note that the lines joining the points are guide to the eye.

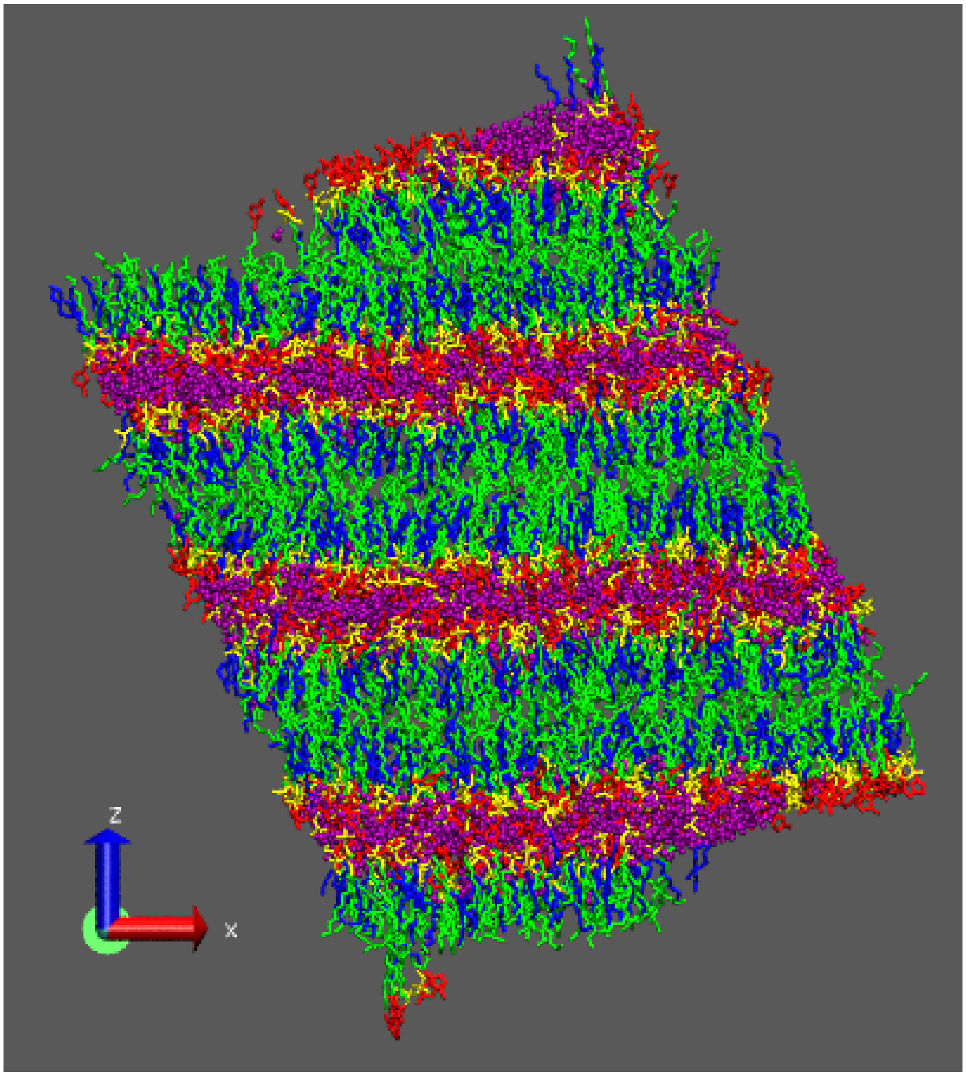

Fig. 5. Morphology of IL:Water mixture system (as seen in Fig 3 (a)) aligned in such a way that polar domains are perpendicular to the z-axis.

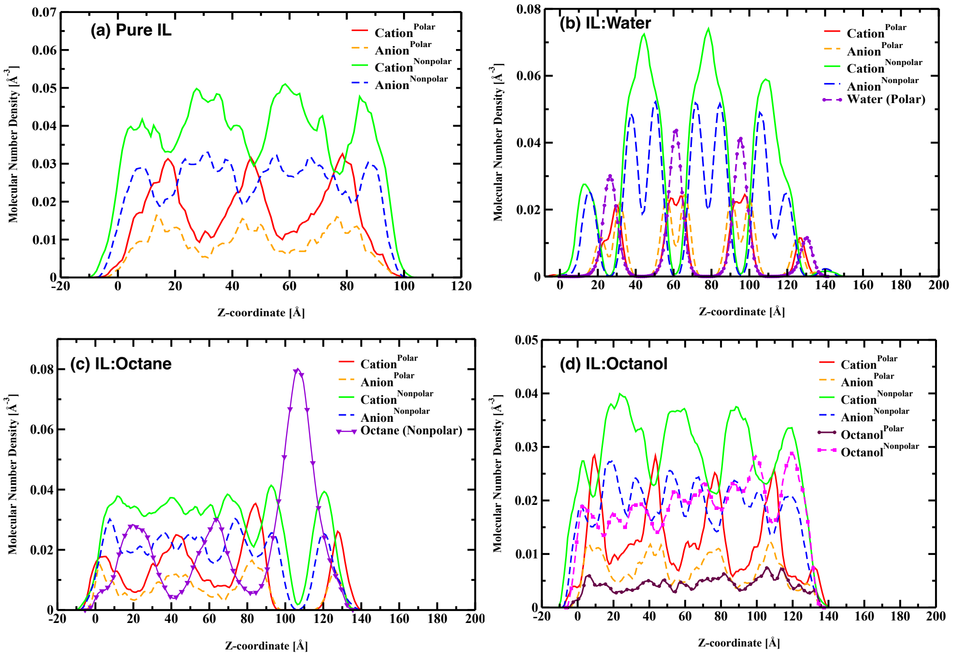

Fig. 6. Molecular number density profiles for (a) pure [C_{12}mim][C_8SO_4], IL (b) IL:Water, (c) IL:Octane. and (d) IL:Octanol systems. Each line represents the molecular number density per unit volume for different groups in the system along a z-coordinate axis

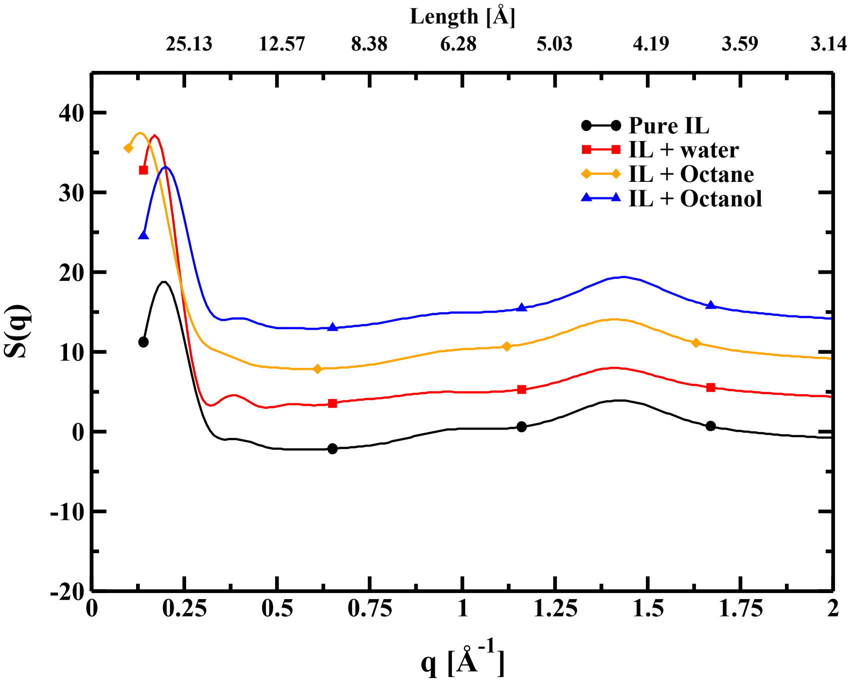

Fig. 7. Total structure factors, S(q), as a function of reciprocal space wavenumber, q [$\AA^{-1}$], on primary abscissa with corresponding real space distance plotted on the secondary abscissa, for pure IL, IL:Water, IL:Octane and IL:Octanol systems at 400 K.

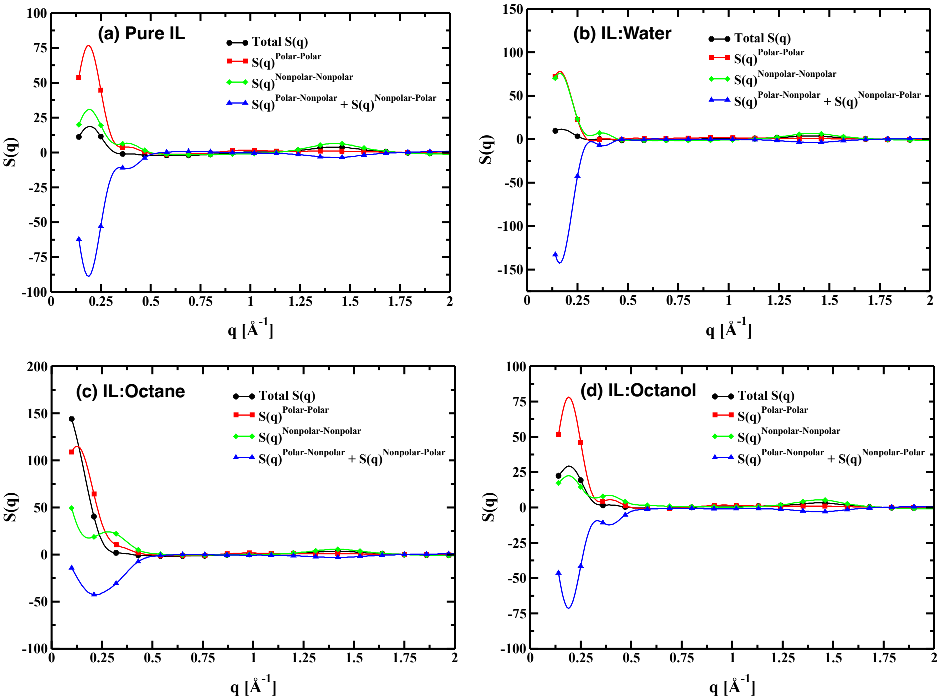

Fig. 8. Total S(q) along with its subcomponents, partial structure factors, for $[C_{12}mim][C_8SO_4]$ ionic liquid defined via polarity partitioning in (a) pure IL, (b) IL:Water, (c) IL:Octane, and (d) IL:Octanol systems at 400 K.

6. acknowledgement

This material is based upon work supported by the National Science Foundation (NSF) Award Number CBET-1706978. The authors gratefully acknowledge partial funding from the Oklahoma State University. Computational resources were provided by the High Performance Computing Center (HPCC) at the Oklahoma State University.

7. Supporting Information

Supporting information file contains structure factors for the ionic liquid-solvent composite system and corresponding polarity partitioning, Voronoi domain count analysis, radial distribution functions, and aggregate size distribution analyses.

1. Canongia Lopes JN, Costa Gomes MF, Pádua AAH, Nonpolar, Polar, and Associating Solutes in Ionic Liquids, *J Phys Chem B* **110**(34):16816–16818, 2006.
2. Triolo A, Russina O, Bleif HJ, Di Cola E, Nanoscale Segregation in Room Temperature Ionic Liquids †, *J Phys Chem B* **111**(18):4641–4644, 2007.
3. Blesic M, Swadźba-Kwaśny M, Belhocine T, Gunaratne HQN, Lopes JNC, Gomes MFC, Pádua AAH, Seddon KR, Rebelo LPN, 1-Alkyl-3-methylimidazolium alkanesulfonate ionic liquids, [CnH2n+1mim][CkH2k+1SO3]: synthesis and physicochemical properties, *Physical Chemistry Chemical Physics* **11**(39):8939–10, 2009.
4. Russina O, Triolo A, Gontrani L, Caminiti R, Xiao D, Hines Jr LG, Bartsch RA, Quitevis EL, Pleckhova N, Seddon KR, Morphology and Intermolecular Dynamics of 1-Alkyl-3-methylimidazolium Bis(Trifluoromethane)SulfonylAmide Ionic Liquids: Structural and Dynamic Evidence of Nanoscale Segregation, *J Phys: Condens Matter* **21**(42):424121–10, 2009.
5. Gontrani L, Russina O, Celso FL, Caminiti R, Annat G, Triolo A, Liquid structure of trihexyltetradecylphosphonium chloride at ambient temperature: an X-ray scattering and simulation study, *The Journal of Physical Chemistry B* **113**(27):9235–9240, 2009.
6. Greaves TL, Kennedy DF, Mudie ST, Drummond CJ, Diversity Observed in the Nanostructure of Protic Ionic Liquids, *The Journal of Physical Chemistry B* **114**(31):10022–10031, 2010.
7. Kashyap HK, Hettige JJ, Annapureddy HVR, Margulis CJ, SAXS anti-peaks reveal the length-scales of dual positive–negative and polar–apolar ordering in room-temperature ionic liquids, *Chemical Communications* **48**(42):5103–5105, 2012.
8. Kashyap HK, Santos CS, Murthy NS, Hettige JJ, Kerr K, Ramati S, Gwon J, Gohdo M, Lall-Ramnarine SI, Wishart JF, Margulis CJ, Castner EW, Structure of 1-alkyl-1-methylpyrrolidinium bis(trifluoromethylsulfonyl)amide ionic liquids with linear, branched, and cyclic alkyl groups., *The Journal of Physical Chemistry B* **117**(49):15328–15337, 2013.
9. Amith WD, Hettige JJ, Castner Jr EW, Margulis CJ, Structures of Ionic Liquids Having Both Anionic and Cationic Octyl Tails: Lamellar Vacuum Interface vs Sponge-Like Bulk Order, *The Journal of Physical Chemistry Letters* **7**(19):3785–3790, 2016.
10. Hettige JJ, Araque JC, Margulis CJ, Bicontinuity and Multiple Length Scale Ordering in Triphilic Hydrogen-Bonding Ionic Liquids, *The Journal of Physical Chemistry B* **118**(44):12706–12716, 2014.
11. Shah JK, Maginn EJ, Molecular dynamics investigation of biomimetic ionic liquids, *FLUID PHASE EQUILIBRIA* **294**(1-2):197–205, 2010.

12. Araque JC, Hettige JJ, Margulis CJ, Modern Room Temperature Ionic Liquids, a Simple Guide to Understanding Their Structure and How It May Relate to Dynamics, *J Phys Chem B* **119**(40):12727–12740, 2015.
13. Shimizu K, Gomes MFC, Pádua AAH, Rebelo LPN, Lopes JNC, Three commentaries on the nano-segregated structure of ionic liquids, *Journal of Molecular Structure: THEOCHEM* **946**(1-3):70–76, 2010.
14. Cammarata L, Kazarian S, Salter P, Welton T, Molecular states of water in room temperature ionic liquids, *Physical Chemistry Chemical Physics* **3**(23):5192–5200, 2001.
15. Saha S, Hamaguchi HO, Effect of water on the molecular structure and arrangement of nitrile-functionalized ionic liquids, *The Journal of Physical Chemistry B* **110**(6):2777–2781, 2006.
16. Rollet AL, Porion P, Vaultier M, Billard I, Deschamps M, Bessada C, Jouvensal L, Anomalous Diffusion of Water in [BMIM][TFSI] Room-Temperature Ionic Liquid, *The Journal of Physical Chemistry B* **111**(41):11888–11891, 2007.
17. Xu Y, Gao Y, Zhang L, Yao J, Wang C, Li H, Microscopic structures of ionic liquids 1-ethyl-3-methylimidazolium tetrafluoroborate in water probed by the relative chemical shift, *Science in China Series B: Chemistry* **53**(7):1561–1565, 2010.
18. Stark A, Zidell AW, Hoffmann MM, Is the ionic liquid 1-ethyl-3-methylimidazolium methanesulfonate [emim][MeSO3] capable of rigidly binding water?, *Journal Of Molecular Liquids* **160**(3):166–179, 2011.
19. Salma U, Plechkova NV, Caminiti R, Gontrani L, The Opposite Effect of Water and N-Methyl-2-Pyrrolidone Cosolvents on the Nanostructural Organization of Ethylammonium Butanoate Ionic Liquid: A Small- and Wide-Angle X-Ray Scattering and Molecular Dynamics Simulations Study, *The Journal of Physical Chemistry B* **121**(26):6399–6407, 2017.
20. Bernardes CES, Minas da Piedade ME, Canongia Lopes JN, The Structure of Aqueous Solutions of a Hydrophilic Ionic Liquid: The Full Concentration Range of 1-Ethyl-3-methylimidazolium Ethylsulfate and Water, *The Journal of Physical Chemistry B* **115**(9):2067–2074, 2011.
21. Bhargava B, Klein M, Initial stages of aggregation in aqueous solutions of ionic liquids: Molecular dynamics studies, *The Journal of Physical Chemistry B* **113**:9499–9505, 2009.
22. Bhargava BL, Klein ML, Formation of Interconnected Aggregates in Aqueous Dicationic Ionic Liquid Solutions, *J Chem Theory Comput* **6**(3):873–879, 2010.
23. Bhargava B, Klein M, Aqueous solutions of imidazolium ionic liquids: molecular dynamics studies, *SOFT MATTER* **5**(18):3475–3480, 2009.
24. Bernardes CES, Shimizu K, Canongia Lopes JN, Solvent effects on the polar network of ionic liquid solutions, *Journal of Physics: Condensed Matter* **27**(19):194116–13, 2015.
25. Bhargava BL, Yasaka Y, Klein ML, Computational Studies of Room Temperature Ionic Liquid-Water Mixtures, *Chem Commun* **47**(22):6228–14, 2011.
26. Nickerson SD, Nofen EM, Chen H, Ngan M, Shindel B, Yu H, Dai LL, A Combined Experimental and Molecular Dynamics Study of Iodide-Based Ionic Liquid and Water Mixtures., *The Journal of Physical Chemistry B* **119**(28):8764–8772, 2015.
27. Zhong X, Fan Z, Liu Z, Cao D, Local Structure Evolution and its Connection to Thermodynamic and Transport Properties of 1-Butyl-3-methylimidazolium Tetrafluoroborate and Water Mixtures by Molecular Dynamics Simulations, *The Journal of Physical Chemistry B* **116**(10):3249–3263, 2012.
28. Feng S, Voth GA, Molecular dynamics simulations of imidazolium-based ionic liquid/water mixtures: Alkyl side chain length and anion effects, *FLUID PHASE EQUI-*

LIBRIA **294**(1-2):148–156, 2010.

29. D'Angelo P, Zitolo A, Aquilanti G, Migliorati V, Using a Combined Theoretical and Experimental Approach to Understand the Structure and Dynamics of Imidazolium-Based Ionic Liquids/Water Mixtures. 2. EXAFS Spectroscopy, *The Journal of Physical Chemistry B* **117**(41):12516–12524, 2013.
30. Ramya KR, Kumar P, Kumar A, Venkatnathan A, Interplay of Phase Separation, Tail Aggregation, and Micelle Formation in the Nanostructured Organization of Hydrated Imidazolium Ionic Liquid, *The Journal of Physical Chemistry B* **118**(29):8839–8847, 2014.
31. Jungnickel C, Łuczak J, Ranke J, Fernández JF, Müller A, Thöming J, Micelle formation of imidazolium ionic liquids in aqueous solution, *Colloids And Surfaces A-Physicochemical And Engineering Aspects* **316**(1-3):278–284, 2008.
32. Yee P, Shah JK, Maginn EJ, State of Hydrophobic and Hydrophilic Ionic Liquids in Aqueous Solutions: Are the Ions Fully Dissociated?, *The Journal of Physical Chemistry B* **117**(41):12556–12566, 2013.
33. Singh AP, Gardas RL, Senapati S, How water manifests the structural regimes in ionic liquids, *SOFT MATTER* **13**:2348–2361, 2017.
34. Widegren
JA, Magee JW, Density, Viscosity, Speed of Sound, and Electrolytic Conductivity for the Ionic Liquid 1-Hexyl-3-methylimidazolium Bis(trifluoromethylsulfonyl)imide and Its Mixtures with Water † **52**(6):2331–2338, 2007.
35. Widegren J, Saurer E, Marsh K, Magee J, Electrolytic conductivity of four imidazolium-based room-temperature ionic liquids and the effect of a water impurity, *Journal of chemical thermodynamics* **37**(6):569–575, 2005.
36. Widegren JA, Laesecke A, Magee JW, The effect of dissolved water on the viscosities of hydrophobic room-temperature ionic liquids, *Chemical Communications* (12):1610–1612, 2005.
37. Seddon K, Stark A, Torres M, Influence of chloride, water, and organic solvents on the physical properties of ionic liquids, *Pure and Applied Chemistry,* Queens Univ Belfast, QUILL Ctr, Belfast BT9 5AG, Antrim, North Ireland, pp. 2275–2287, 2000.
38. Crosthwaite JM, Aki SNVK, Maginn EJ, Brennecke JF, Liquid phase behavior of imidazolium-based ionic liquids with alcohols: effect of hydrogen bonding and non-polar interactions, *FLUID PHASE EQUILIBRIA* **228-229**:303–309, 2005.
39. Freire MG, Carvalho PJ, Gardas RL, Marrucho IM, Santos LMNBF, Coutinho JAP, Mutual Solubilities of Water and the [$C_n$nmim][Tf_2N] Hydrophobic Ionic Liquids, *The Journal of Physical Chemistry B* **112**(6):1604–1610, 2008.
40. Chapeaux A, Simoni LD, Stadtherr MA, Brennecke JF, Liquid Phase Behavior of Ionic Liquids with Water and 1-Octanol and Modeling of 1-Octanol/Water Partition Coefficients, *Journal of Chemical & Engineering Data* **52**(6):2462–2467, 2007.
41. Anthony J, Maginn E, Brennecke J, Solution thermodynamics of imidazolium-based ionic liquids and water, *The Journal of Physical Chemistry B* **105**(44):10942–10949, 2001.
42. Raabe G, Köhler J, Thermodynamical and structural properties of binary mixtures of imidazolium chloride ionic liquids and alcohols from molecular simulation, *The Journal of Chemical Physics* **129**:144503, 2008.
43. Jahangiria S, Taghikhanib M, Behnejada H, Ahmadib S, Theoretical investigation of imidazolium based ionic liquid/alcohol mixture: a molecular dynamic simulation, *Molecular Physics* **106**(8):1015–1023, 2008.
44. Carrete J, Méndez-Morales T, Cabeza Ó, Lynden-Bell RM, Gallego LJ, Varela LM, Investigation of the Local Structure of Mixtures of an Ionic Liquid with Polar Molecular

Species through Molecular Dynamics: Cluster Formation and Angular Distributions, *The Journal of Physical Chemistry B* **116**(20):5941–5950, 2012.

45. Greaves TL, Kennedy DF, Kirby N, Drummond CJ, Nanostructure changes in protic ionic liquids (PILs) through adding solutes and mixing PILs, *Physical Chemistry Chemical Physics* **13**(30):13501, 2011.
46. Russina O, Sferrazza A, Caminiti R, Triolo A, Amphiphile Meets Amphiphile: Beyond the Polar–Apolar Dualism in Ionic Liquid/Alcohol Mixtures, *The Journal of Physical Chemistry Letters* pp. 1738–1742, 2014.
47. González EJ, Navarro P, Larriba M, García J, Rodríguez F, A comparative study of pure ionic liquids and their mixtures as potential mass agents in the separation of hydrocarbons, *Journal Of Molecular Liquids* **222**(C):118–124, 2016.
48. Navarro P, Larriba M, García J, Rodríguez F, Vapor–Liquid Equilibria for (n-Hexane, n-Octane, Cyclohexane, or 2,3-Dimethylpentane) + Toluene + [4empy][Tf 2N] (0.3) + [emim][DCA] (0.7) Mixed Ionic Liquids **61**(7):2440–2449, 2016.
49. Navarro P, Larriba M, García J, Rodríguez F, Vapor-liquid equilibria for n-heptane + (benzene, toluene, p-xylene, or ethylbenzene) + [4empy][Tf2N] (0.3) + [emim][DCA] (0.7) binary ionic liquid mixture, *FLUID PHASE EQUILIBRIA* **417**(C):41–49, 2016.
50. Green BD, Badini AJ, O'Brien RA, Davis JH, West KN, Liquid-liquid equilibria of binary mixtures of a lipidic ionic liquid with hydrocarbons., *Physical Chemistry Chemical Physics* **18**(4):2459–2467, 2016.
51. Canongia Lopes JN, Pádua AAH, Molecular Force Field for Ionic Liquids III: Imidazolium, Pyridinium, and Phosphonium Cations; Chloride, Bromide, and Dicyanamide Anions, *J Phys Chem B* **110**(39):19586–19592, 2006.
52. Canongia Lopes JN, Pádua AAH, Shimizu K, Molecular Force Field for Ionic Liquids IV: Trialkylimidazolium and Alkoxycarbonyl-Imidazolium Cations; Alkylsulfonate and Alkylsulfate Anions, *J Phys Chem B* **112**(16):5039–5046, 2008.
53. Berendsen HJC, Grigera JR, Straatsma TP, The Missing Term in Effective Pair Potentials, *J Phys Chem* **91**(24):6269–6271, 1987.
54. Soper AK, Bruni F, Ricci MA, Site–Site pair Correlation Functions of Water from 25 to 400^{o}C: Revised Analysis of New and Old Diffraction Data, *J Chem Phys* **106**(1):247–254, 1997.
55. Mark P, Nilsson L, Structure and Dynamics of the TIP3P, SPC, and SPC/E Water Models at 298 K, *J Phys Chem A* **105**(43):9954–9960, 2001.
56. Kapoor U, Shah JK, Globular, Sponge-like to Layer-like Morphological Transition in 1-*n*-Alkyl-3-Methylimidazolium Octylsulfate Ionic Liquid Homologous Series, *J Phys Chem B* **under review**, 2017.
57. Lindahl E, Hess B, van der Spoel D, GROMACS 3.0: A Package for Molecular Simulation and Trajectory Analysis, *Molec Model Ann* **7**(8):306–317, 2001.
58. Abraham MJ, van der Spoel D, Lindahl E, Hess B, , the GROMACS development team, GROMACS User Manual Version 5.0.4, www.gromacs.org, *J Mol Model* , 2014.
59. Martínez L, Andrade R, Birgin EG, Martínez JM, PACKMOL: A Package for Building Initial Configurations for Molecular Dynamics Simulations, *J Comput Chem* **30**(13):2157–2164, 2009.
60. Shimizu K, Bernardes CES, Triolo A, Canongia Lopes JN, Nano-Segregation in Ionic liquids: Scorpions and Vanishing Chains, *Phys Chem Chem Phys* **15**(38):16256–7, 2013.
61. Giorgino T, Computing 1-D Atomic Densities in Macromolecular Simulations: The Density Profile Tool for VMD, *Computer Physics Communications* **185**(1):317–322, 2014.
62. Brehm M, Kirchner B, TRAVIS - A Free Analyzer and Visualizer for Monte Carlo

and Molecular Dynamics Trajectories, *J Chem Inf Model* **51**(8):2007–2023, 2011.

63. Brehm M, Weber H, Thomas M, Hollóczki O, Kirchner B, Domain Analysis in Nanostructured Liquids: A Post-Molecular Dynamics Study at the Example of Ionic Liquids, *Chem Phys Chem* **16**(15):3271–3277, 2015.
64. Humphrey W, Dalke A, Schulten K, VMD: Visual Molecular Dynamics, *J Mol Graph* **14**:33–38, 1996.
65. McGibbon RT, Beauchamp KA, Harrigan MP, Klein C, Swails JM, Hernández CX, Schwantes CR, Wang LP, Lane TJ, Pande VS, MDTraj: A Modern Open Library for the Analysis of Molecular Dynamics Trajectories, *Biophysj* **109**(8):1528–1532, 2015.
66. Bernardes CES, AGGREGATES: Finding Structures in Simulation Results of Solutions, *J Comput Chem* **38**(10):753–765, 2017.
67. Canongia Lopes JNA, Pádua AAH, Nanostructural Organization in Ionic Liquids, *J Phys Chem B* **110**(7):3330–3335, 2006.
68. Annapureddy HVR, Kashyap HK, De Biase PM, Margulis CJ, What is the Origin of the Prepeak in the X-ray Scattering of Imidazolium-Based Room-Temperature Ionic Liquids?, *J Phys Chem B* **114**(50):16838–16846, 2010.
69. Triolo A, Russina O, Fazio B, Triolo R, Di Cola E, Morphology of 1-Alkyl-3-methylimidazolium Hexafluorophosphate Room Temperature Ionic Liquids, *Chem Phys Lett* **457**(4-6):362–365, 2008.
70. Macchiagodena M, Gontrani L, Ramondo F, Triolo A, Caminiti R, Liquid Structure of 1-Alkyl-3-methylimidazolium-Hexafluorophosphates by Wide Angle X-Ray and Neutron Scattering and Molecular Dynamics, *J Chem Phys* **134**(11):114521–16, 2011.
71. Bodo E, Chiricotto M, Caminiti R, Structure of Geminal Imidazolium Bis(trifluoromethylsulfonyl)imide Dicationic Ionic Liquids: A Theoretical Study of the Liquid Phase, *J Phys Chem B* **115**(49):14341–14347, 2011.
72. Shimizu K, Bernardes CES, Canongia Lopes JN, Structure and Aggregation in the 1-Alkyl-3-Methylimidazolium Bis(trifluoromethylsulfonyl)imide Ionic Liquid Homologous Series, *J Phys Chem B* **118**(2):567–576, 2014.
73. Bhargava BL, Klein ML, Molecular Dynamics Studies of Cation Aggregation in the Room Temperature Ionic Liquid [C_{10}mim][Br] in Aqueous Solution †, *J Phys Chem A* **113**(10):1898–1904, 2009.
74. Firestone MA, Rickert PG, Seifert Sn, Dietz ML, Anion Effects on Ionogel Formation in N,N'-Dialkylimidazolium-Based Ionic Liquids, *Inorganica Chimica Acta* **357**(13):3991–3998, 2004.
75. Greaves TL, Kennedy DF, Weerawardena A, Tse NMK, Kirby N, Drummond CJ, Nanostructured Protic Ionic Liquids Retain Nanoscale Features in Aqueous Solution While Precursor Brønsted Acids and Bases Exhibit Different Behavior, *J Phys Chem B* **115**(9):2055–2066, 2011.
76. Abe H, Imai Y, Takekiyo T, Yoshimura Y, Deuterated Water Effect in a Room Temperature Ionic Liquid: N, N-Diethyl- N-methyl- N-2-methoxyethyl Ammonium Tetrafluoroborate, *J Phys Chem B* **114**(8):2834–2839, 2010.
77. Aparicio S, Alcalde R, Atilhan M, Experimental and Computational Study on the Properties of Pure and Water Mixed 1-Ethyl-3-methylimidazolium l-(+)-Lactate Ionic Liquid, *J Phys Chem B* **114**(17):5795–5809, 2010.
78. Yoshimura Y, Goto T, Abe H, Imai Y, Existence of Nearly-Free Hydrogen Bonds in an Ionic Liquid, N, N-Diethyl- N-methyl- N-(2-methoxyethyl) Ammonium Tetrafluoroborate-Water at 77 K, *J Phys Chem B* **113**(23):8091–8095, 2009.
79. Blesic M, Lopes JNC, Gomes MFC, Rebelo LPN, Solubility of Alkanes, Alkanols and their Fluorinated Counterparts in Tetraalkylphosphonium Ionic Liquids, *Phys Chem Chem Phys* **12**(33):9685–8, 2010.

80. Greaves TL, Drummond CJ, Solvent Nanostructure, the Solvophobic Effect and Amphiphile Self-Sssembly in Ionic Liquids, *Chem Soc Rev* **42**(3):1096–1120, 2013.
81. Cruz C, Heinrich B, Ribeiro AC, Bruce DW, Guillon D, Structural Study of Smectic A Phases in Homologous Series of N-Alkylpyridinium Alkylsulphates, *Liq Cryst* **27**(12):1625–1631, 2000.
82. Gennes Pd, Prost J, *The Physics of Liquid Crystals*Clarendon Press: Oxford, Clarendon Press: Oxford, Clarendon Press: Oxford, 1995.
83. Saupe, A, Recent Results in the Field of Liquid Crystals, *Angew Chem Internat Edit* **7**(2):97–112, 1968.
84. Gennes Pd, *Scaling Concepts in Polymer Physics*Cornell University Press: Oxford, Cornell University Press: Oxford, Cornell University Press: Oxford, 1979.
85. Lemaire BJ, Panine P, Gabriel JCP, Davidson P, The Measurement by SAXS of the Nematic Order Parameter of Laponite Gels, *Europhys Lett* **59**(1):55–61, 2002.
86. Amith WD, Hettige JJ, Castner Jr EW, Margulis CJ, Structures of Ionic Liquids Having Both Anionic and Cationic Octyl Tails: Lamellar Vacuum Interface vs Sponge-Like Bulk Order, *J Phys Chem Lett* **7**(19):3785–3790, 2016.
87. Hettige JJ, Amith WD, Castner Jr EW, Margulis CJ, Ionic Liquids with Symmetric Diether Tails: Bulk and Vacuum-Liquid Interfacial Structures, *J Phys Chem B* **121**(1):174–179, 2017.
88. Ji Y, Shi R, Wang Y, Saielli G, Effect of the Chain Length on the Structure of Ionic Liquids: from Spatial Heterogeneity to Ionic Liq. Cryst., *J Phys Chem B* **117**(4):1104–1109, 2013.
89. Guo H, Kremer K, Molecular Dynamics Simulation of the Phase Behavior of Lamellar Amphiphilic Model Systems, *J Chem Phys* **119**(17):9308–9320, 2003.
90. Brown PJ, Fox AG, Maslen EN, O?Keefe MA, Willis TM, International Tables for Crystallography, *Prince, E, Ed International Union of Crystallography: Dordrecht,The Netherlands* **C**:554–595, 2004.
91. Lorch E, Neutron Diffraction by Germania, Silica and Radiation-Damaged Silica Glasses, *J Phys C: Solid State Phys* **2**(8):229–237, 1969.
92. Bernardes CES, Shimizu K, Lobo Ferreira AIMC, Santos LMNBF, Canongia Lopes JN, Structure and Aggregation in the 1,3-Dialkyl-imidazolium Bis(trifluoromethylsulfonyl)imide Ionic Liquid Family: 2. From Single to Dou$[C_{12}mim]^+$ Long Alkyl Side Chains, *J Phys Chem B* **118**(24):6885–6895, 2014.
93. Shimizu K, Lopes JNC, Probing the Structural Features of the 1-Alkyl-3-methylimidazolium Hexafluorophosphate Ionic Liquid Series Using Molecular Dynamics Simulations, *J Mol Liq* **210**(PB):257–263, 2015.
94. Shimizu K, Freitas AA, Lopes JNC, Structural Characterization of the [CnC1im][C4F9SO3] Ionic Liquid Series: Alkyl Versus Perfluoroalkyl Side Chains, *J Mol Liq* pp. 1–7, 2016.
95. Kashyap HK, Margulis CJ, (Keynote) Theoretical Deconstruction of the X-ray Structure Function Exposes Polarity Alternations in Room Temperature Ionic Liquids, *ECS Transactions* **50**(11):301–307, 2013.